Bulk and surface phase transitions in the three-dimensional $O(4)$ spin model

Youjin Deng

Department of Physics, 4 Washington Square Place, New York University, New York, New York 10003, USA
(Received 20 February 2006; published 19 May 2006)

We investigate the $O(4)$ spin model on the simple-cubic lattice by means of the Wolff cluster algorithm. Using the toroidal boundary condition, we locate the bulk critical point at coupling $K_c=0.935\,856(2)$, and determine the bulk thermal magnetic renormalization exponents as $y_t=1.337\,5(15)$ and $y_h=2.482\,0(2)$, respectively. The universal ratio $Q=\langle m^2\rangle^2/\langle m^4\rangle$ is also determined as 0.9142(1). The precision of these estimates significantly improves over that of the existing results. Then, we simulate the critical $O(4)$ model with two open surfaces on which the coupling strength K_1 can be varied. At the ordinary transitions, the surface magnetic exponent is determined as $y_{h1}^{(o)}=1.020\,2(12)$. Further, we find a so-called special surface transition at $\kappa=K_1/K-1=1.258(20)$. At this point, the surface thermal exponent $y_{t1}^{(s)}$ is rather close to zero, and we cannot exclude that the corresponding surface transition is Kosterlitz-Thouless-like. The surface magnetic exponent is $y_{h1}^{(s)}=1.816(2)$.

I. INTRODUCTION

The classical $O(N)$ spin model, characterized by a N-component order parameter, plays a significant role in the field of statistical physics and condensed-matter physics. It is known that this model can describe the universal critical behavior of many physical systems. In the limit $N\to0$, the $O(N)$ model reduces to the self-avoiding random walk, which is an important theoretical model in the polymer science. The $N=1$ case corresponds to the Ising model, and describes phase transitions ranging from the liquid-vapor to the magnetic transition in uniaxial (anti-)ferromagnets. The universal critical behavior of the helium superfluid transition and of the Meissner transition in type II superconductors is believed to belong to the XY ($N=2$) universality class. For $N=3$, one has the Heisenberg model for the isotropic magnets. In three dimensions, the $O(4)$ model is related to the finite-temperature phase transition in QCD with two light flavors. The $O(5)$ model is relevant to the so-called $SO(5)$ theory of high T_c superconductivity. The $N=6$ case describes the chiral phase transition in QCD with two flavors and two colors.

Exact results about the critical behavior of the three-dimensional $O(N)$ model are scarce; investigations mainly rely on approximation techniques. These include the high-temperature series expansion, the field-theoretical formulation of the renormalization group, and the Monte Carlo simulations. The thermal and magnetic critical exponents have been determined for many values of N, including all the integers in range $0\leqslant N\leqslant6$ [1–12] and $N=32$ and $N=64$ [13]. For a recent review, see Ref. [14].

In this work we focus on the $O(4)$ model on the simple-cubic lattice. Our goal is twofold: to improve the precision of the bulk critical point and provide an independent and careful determination of the bulk critical exponents, and then to investigate the surface phase transitions by simulating the critical model with open surfaces.

On the $L\times L\times L$ simple-cubic lattice with periodic boundary conditions in all the directions (namely, the toroi-

dal boundary condition), the Hamiltonian of the $O(4)$ model in zero magnetic field reads

$$\mathcal{H}/k_BT=-K\sum_{\{ij\}}\vec{s}_i\cdot\vec{s}_j,\qquad(1)$$

where K is the coupling strength between nearest-neighbor lattice sites. The dynamic variable $\vec{s}$ is a unit vector of $N=4$ components. To our knowledge, the best estimate of the critical coupling of this model is $K_c=0.935\,90(5)$ [15]. The thermal and magnetic exponents were determined as $y_t=1.335(4)$ and $y_h=2.4817(5)$ [7]. The precision of the estimated critical point is rather limited in comparison with those of the estimated critical points for the Ising, XY, and Heisenberg cases: $K_c(N=1)=0.221\,654\,55(3)$ [2], $K_c(N=2)=0.454\,165\,9(10)$ [3,16,17], and $K_c(N=3)=0.693\,003(2)$ [3,16,17]. It might not be sufficient for our aim of studying surface effects at the bulk criticality.

Surface effects on the $O(N)$ model, particularly on the Ising model, have been extensively investigated. Near the bulk critical points, owning to the long-range bulk correlations, surface effects can be significant and, in many cases, they cannot be neglected. The surfaces can display critical phenomena that differ from the bulk critical behavior; for each bulk criticality, different surface universality classes can exist. For a review, see Refs. [18–20], and for more recent work see Refs. [17,21,22]

Here, we shall review surface phase transitions on the simple-cubic Ising model with periodic and free boundary conditions in the xy plane and along the z direction, respectively. Namely, for a finite system with linear size L, there are two open surfaces at $z=1$ and $z=L$. The interaction strengths K_1 on the surfaces can assume different values from those K in the bulk. The Hamiltonian of this Ising model can then be written into two parts: a bulk term proportional to the volume of the system and a surface term proportional to the surface areas, i.e.,

$$\mathcal{H}/k_BT=-K\sum_{\langle ij\rangle}{}^{(b)}s_is_j-K_1\sum_{\langle lm\rangle}{}^{(s)}s_ls_m,\qquad(2)$$
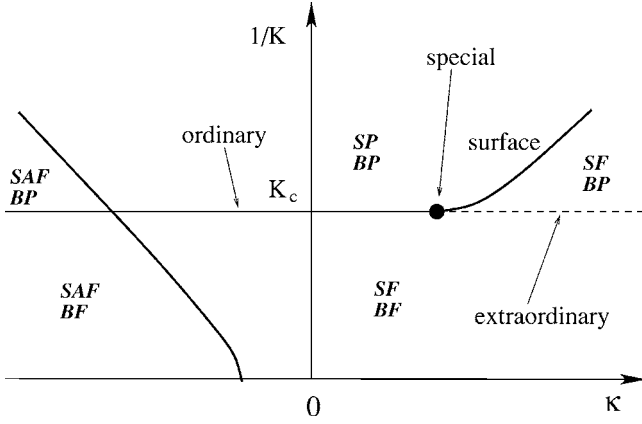
FIG. 1. Schematic phase diagram for the three-dimensional Ising model with ferromagnetic bulk couplings $K > 0$. The bulk transition is $K = K_c$, and the the bulk state is denoted as *BF* for a ferromagnet and *BP* for a paramagnet. The surface phases are labeled as *SF*, *SP*, and *SAF* for the ferro-, para-, and antiferromagnets, respectively. The symbol $\kappa = K_1/K$ is the ratio of the surface over the bulk coupling constant.

where the first sum accounts for the bulk and the second sum involves the spins on the open surfaces. The phase diagram of the model (2) is then sketched in Fig. 1. The critical line $K = K_c$ separates the bulk paramagnetic and ferromagnetic states, denoted as BP and BF in Fig. 1, respectively. When the surface coupling K_1 is varied, the local behavior on and near the surfaces can be significantly modified. For a paramagnetic bulk $K < K_c$, the surfaces can behave as an antiferromagnet (SAF), a ferromagnet (SF), and a paramagnet (SP), depending on the sign and the strength of K_1. The corresponding phase transitions occurring on the surfaces are referred to as the 'surface "transitions"' and they are represented by the solid curved lines in Fig. 1. Due to the absence of long-ranged bulk correlations, these surface transitions display critical behavior as the two-dimensional Ising model with anti-or ferromagnetic couplings, $K_1 < 0$ or $K_1 > 0$, respectively. For the surface couplings $K_1 < 0$, because the bulk and surface couplings have different signs, the line of surface transitions, which is in the two-dimensional Ising universality class, extends to the zero temperature. However, for ferromagnetic surface couplings $K_1 > 0$, the surface critical line terminates at the bulk criticality in a "special" critical point $(K_c, K_{1c}^{(s)})$. At this point, the surface critical correlations coincide with the diverging bulk correlation lengths. Thus, the point $(K_c, K_{1c}^{(s)})$ acts as a "multicritical" point, and the phase transition is referred to as the 'special transition.' For $K_1 < K_{1c}^{(s)}$, when K is varied, both the surfaces and the bulk simultaneously undergo a phase transition at $K = K_c$. In this case, the critical correlations on the surfaces arise from the diverging bulk correlation length, and the phase transition is named the "ordinary transition." For the larger coupling $K_1 > K_{1c}^{(s)}$, however, since the surfaces become ferromagnetic at a smaller coupling $K < K_c$, the bulk transition at $K = K_c$ has to occur in the presence of spontaneous long-ranged surface order, and the transition is referred to as the "extraordinary transition." Nevertheless, the surfaces still display some critical behavior owing to diverging bulk cor-

TABLE I. Description of the simulations of the $O(4)$ model. The table lists the simulation length in millions of samples (No. MS), and the number of Wolff clusters (No. Wc/S) between subsequent samples, for each system size L. The average size of a Wolff cluster at $K = 0.935\,870$ is also presented, which is in the unit of the lattice volume. The simulations were performed for several values of K in a range ΔK about the critical point K_c. According to Ref. [6], the autocorrelation time of the Wolff cluster simulations is about $\tau \approx 2.0$, in the unit of updates of the whole spins on the lattice. The approximate number of independent samples can then be calculated from No. MS, No.Wc/S, and S_w.

L	No. MS	No. Wc/S	S_w	ΔK
5	240	2	0.162 32(4)	0.024
6	240	3	0.134 67(3)	0.024
7	240	3	0.114 96(2)	0.024
8	240	4	0.100 22(2)	0.024
9	240	4	0.088 78(2)	0.024
10	240	5	0.079 60(2)	0.012
12	240	6	0.065 96(1)	0.012
14	240	7	0.056 26(1)	0.012
16	240	8	0.049 01(1)	0.008
20	160	10	0.038 912(8)	0.004
24	160	12	0.032 236(7)	0.004
32	120	16	0.023 914(6)	0.002
40	120	20	0.018 991(5)	0.002
48	40	24	0.015 735(4)	0
64	120	32	0.011 674(3)	0.0004
96	40	48	0.007 672(2)	0.0003
150	6	75	0.004 840(3)	0

relation lengths. At the ordinary, the special, and the extraordinary surface transitions, the scaling behavior of the magnetic correlations on the surfaces is governed by different exponents; we shall denote them as $y_{h1}^{(o)}$, $y_{h1}^{(s)}$, and $y_{h1}^{(e)}$, respectively. In addition, the special transition has a relevant thermal surface exponent $y_{t1}^{(s)}$.

From the phase diagram in Fig. 1, it is clear that the occurance of the multicritical point, i.e., the special transition, is closely related to the existence of the line of surface phase transitions in the bulk paramagnetic region $K < K_c$. Since the two-dimensional $O(N)$ model with $N > 2$ does not undergo phase transitions at nonzero temperature, the line of surface transitions does not exist in the three-dimensional $O(N)$ model. It may then seem self-evident that the special and the extraordinary transitions do not exist either, and thus that only the ordinary transitions remain on the surfaces. However, such a statement does not agree with some recent studies of the Heisenberg model in three dimensions. It was reported that, at the bulk criticality, the surface magnetic exponents depend on the ratio K_1/K for $K_1/K \geq 2.0$ [23]. Further, in Ref. [17], substantial evidence was found for the existence of a special surface transition. It seems then desirable to provide additional investigations about the existence of a special surface transition for the three-dimensional $O(N)$ model for $N > 2$.
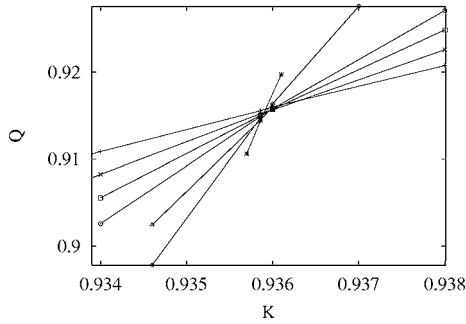
FIG. 2. Binder ratio Q in range $0.934 \leqslant K \leqslant 0.938$. The data points $+$, $\times$, $\square$, $\circ$, $\triangle$, $\diamond$, and $*$ represent system sizes $L=12$, 16, 20, 24, 32, 40, and 64, respectively. The error bars of the data are smaller than the point sizes. The lines, which simply connect data points for each L, are just for illustration purpose.

The organization of the present paper is as follows. Section II generates and analyzes high-precision Monte Carlo data for the $O(4)$ model near the bulk critical point. A comparison of our estimates for various parameters and the existing results is given. In Sec. III, simulations were carried out for several values of K_1/K. We determine the surface magnetic exponent at the ordinary phase transitions, and find substantial evidence for the existence of a special surface transition.

II. BULK CRITICALITY OF THE $O(4)$ MODEL

We study the $O(4)$ model on the $L \times L \times L$ simple-cubic lattice, as described by Eq. (1); periodic boundary conditions were applied in all the x, y, and z directions.

A. Simulation method and sampled quantities

The simulations used a version of the Wolff cluster algorithm [24,25]. The Cartesian components, s^x, s^y, s^z, and s^w, of the spin vectors are stored in computer memory; they satisfied $(s^x)^2+(s^y)^2+(s^z)^2+(s^w)^2=1$.[1] A Wolff cluster is constructed on the basis of the Cartesian component s^w, with bond-occupation probability $p=\max[0, 1-\exp(-2s_i^w s_j^w)]$ for a pair of nearest-neighbor sites. The spin components s^w in the Wolff cluster are then inverted. The simulation consists of a large number of cycles, each of which contains several Wolff steps and a data sampling procedure. Since the cluster flips do not change the absolute values of the spin components, each cycle also includes a random rotation of the whole system of spin vectors.

Simulations were carried out near $K=0.935\,857$, which is rather close to the critical point determined later. The details of the simulations are described in Table I. According to Ref. [6], the dynamical exponent of the Wolff cluster simulation of the $O(4)$ model is very close to zero, and the autocorrelation time is around $\tau \approx 2$. Thus, the approximate number of independent samples can be estimated from Table I.

TABLE II. Numerical data for specific-heat C, susceptibility χ, Binder ratio Q, and quantity Q_p at $K=0.935\,857$.

L	C	χ	Q	Q_p
5	2.210(2)	27.726(6)	0.918 22(6)	0.820(2)
6	2.341(2)	39.943(7)	0.917 50(6)	1.051(2)
7	2.477(2)	54.29(1)	0.916 82(6)	1.296(3)
8	2.531(2)	70.78(1)	0.916 48(6)	1.553(3)
9	2.600(2)	89.38(2)	0.916 23(6)	1.813(3)
10	2.664(2)	110.09(2)	0.915 91(6)	2.094(4)
12	2.761(2)	157.77(3)	0.915 55(6)	2.679(4)
14	2.835(2)	213.85(3)	0.915 37(6)	3.286(8)
16	2.905(2)	278.18(6)	0.915 19(6)	3.934(9)
20	3.000(3)	431.8(1)	0.915 05(6)	5.28(1)
24	3.073(3)	618.2(1)	0.914 89(6)	6.74(1)
32	3.187(3)	1087.2(2)	0.914 63(6)	9.95(2)
40	3.264(3)	1687.0(3)	0.914 57(6)	13.43(3)
48	3.327(4)	2414.2(5)	0.914 51(6)	17.04(5)
64	3.412(4)	4248.7(8)	0.914 40(6)	25.2(1)
96	3.517(6)	9422(3)	0.914 43(8)	43.2(2)
150	3.626(8)	422674(12)	0.914 5(1)	77.6(5)

Various quantities were sampled during the simulations, including the magnetization density $\vec{m}=\frac{1}{L^d}\Sigma_i\vec{s}_i$, and the second and the fourth moments m^2 and m^4. On this basis, the Binder ratio is defined as

$$Q = \frac{\langle m^2 \rangle^2}{\langle m^4 \rangle}. \tag{3}$$

At criticality, the value of Q is universal. It is well accepted that ratio Q is a very good candidate to locate phase transitions in Monte Carlo studies of statistical models.

We also sampled the nearest-neighbor correlation functions, which is an energy-like quantity, as

$$e = \frac{1}{L^d}\sum_{\{ij\}} \vec{s}_i\vec{s}_j, \tag{4}$$

where the sum is over all pairs of nearest-neighbor sites. The specific heat is then defined as $C=L^d(\langle e^2 \rangle - \langle e \rangle^2)$.

We further measured a quantity Q_p, which correlates the magnetization distribution and the energy density, as

$$Q_p = L^d \left[\frac{2\langle em^2 \rangle}{\langle m^2 \rangle} - \frac{\langle em^4 \rangle}{\langle m^4 \rangle} - \langle e \rangle \right]. \tag{5}$$

This quantity can be obtained by differentiating the Binder ratio Q with respect to the coupling strength K. It reflects the slope of the Binder ratio Q at criticality.

B. Simulations and analyses

The numerical data generated by the Wolff cluster simulations were analyzed by the finite-size scaling theory.

The finite-size scaling behavior of quantities defined in the previous subsection can be obtained by differentiating the
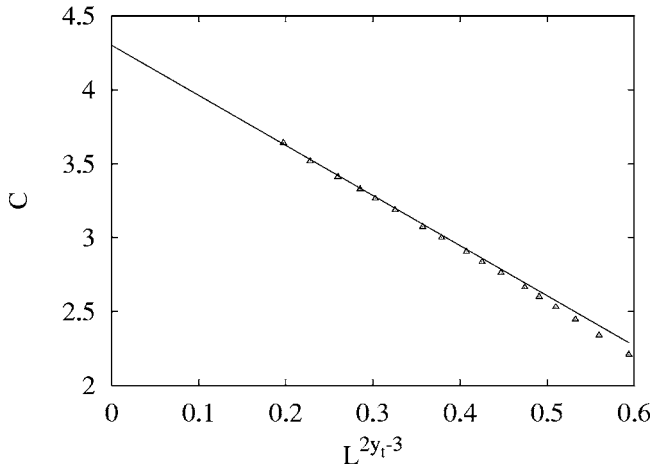
---

[1]The x, y, z, and w directions of the spin vector should not be confused with the spatial dimensions.

FIG. 3. Specific heat C at $K=0.935\,857$ vs L^{2y_t-3}. Exponent y_t was fixed at $y_t=1.337$. The error bars of the data are in the order of the point sizes.

FIG. 5. Quantity Q_p at $K=0.935\,857$ vs L^{y_t}. Exponent y_t was fixed at $y_t=1.337$. The error bars of the data are in the order of the point sizes.

free energy density with respect to appropriate scaling fields. For instance, the leading behavior of the Binder ratio near criticality behaves as

$$Q(K,L) = Q(tL^{y_t}), \qquad (6)$$

where $t \approx (K-K_c)$ is the thermal scaling field, and the right-hand side of Eq. (6) is a universal function. Taking into account finite-size corrections, Taylor expansion of Eq. (6) leads to

$$Q(K,L) = Q_c + \sum_{k=1}^{m} (K-K_c)^k L^{ky_t} + b_i L^{y_i} + b_2 L^{y_2}$$
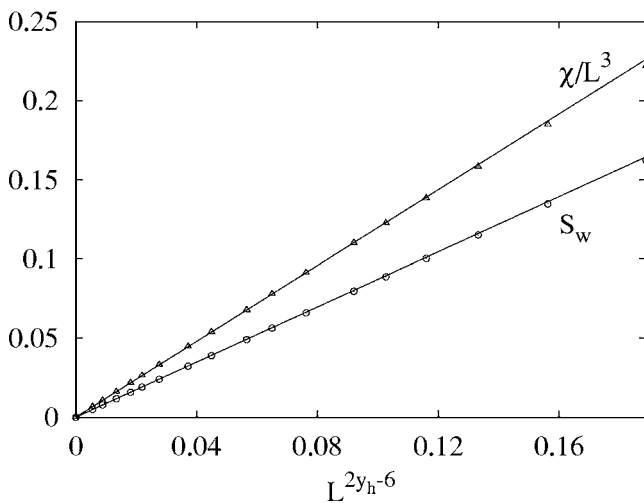$$+ c(K-K_c)L^{y_i+y_t} + \cdots \qquad (7)$$

FIG. 4. Quantities χ/L^3 and S_w at $K=0.935\,857$ vs L^{2y_h-6}. Exponent y_h was fixed at $y_h=2.482$. The error bars of the data are smaller than the point sizes. This figure implies that the scaling behavior of the Wolff-cluster size is indeed governed by the magnetic exponent y_h.
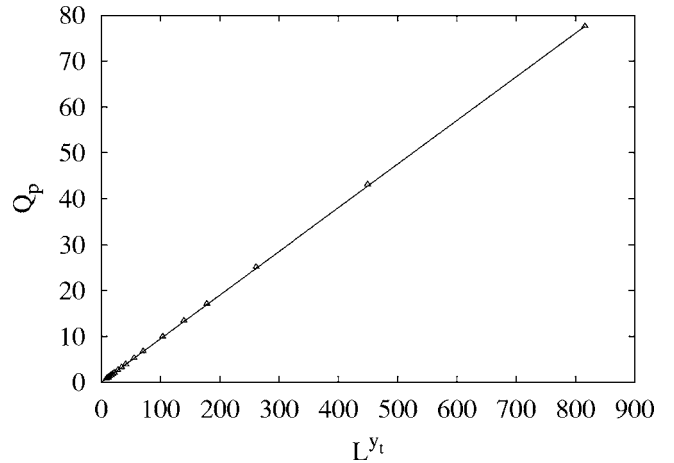
where m is an integer and symbol $\cdots$ means that more terms can be generated. For instance, one can include further finite-size corrections or a term like $n(K-K_c)^2 L^{y_t}$; the latter accounts for the fact that the scaling field t is a nonlinear function of $(K-K_c)$. The term with amplitude b_i comes from the least irrelevant scaling field, of which the exponent was determined as $y_i=-0.796$ in Refs. [4,26]. In addition, it is known that subleading corrections may exist and play a significant role in the finite-size scaling analysis. These corrections can arise from various sources: from the regular part of the free energy, from the second derivative of the free energy with respect to the least irrelevant scaling field, or from the subleading irrelevant scaling field. The first type of subleading corrections has exponent $y_r=d-2y_h \approx -1.96$, as determined later, and the second has $2y_i \approx =-1.6$. It was shown [27] that, for the three-dimensional $O(N)$ model with $N=1,2,3$, the subleading scaling field has exponent about -1.8. Thus, one might expect that such a correction exponent also exists in the $O(4)$ model. Nevertheless, since one does not know how much these finite-size corrections contribute from *a priori* argument, we simply describe them by a single term $b_2 L^{y_2}$. The term with c describes the "mixed" effect of the thermal scaling field and the irrelevant scaling field. The detailed derivation of Eq. (7) can be found in Ref. [2] and references therein.

The Monte Carlo data for Q were fitted by Eq. (7) on the basis of the least-squares criterion. For an illustration, parts of the Q data are shown in Fig. 2. The exponent y_i was left to be determined by the fit. We found that all the data can be described by Eq. (7) with $m=2$. Finite-size corrections are well accounted for by a single term $b_i L^{y_i}$ with amplitude $b_i=0.027(2)$ and exponent $y_i=-1.19(6)$. The value of y_i is not consistent with the earlier determination $y_i=-0.796$ [26]. In Ref. [3], it was determined that $y_i=-1.85(21)$, which is also much smaller than $y_i=-0.796$. A possible scenario for this inconsistency can be that the amplitude for leading corrections is quite small and the estimated exponent $y_i=-1.29(6)$ is owing to a effective mixture of various types of corrections. Various fits have been tried; for instance, we

TABLE III. Results for the critical exponents y_t and y_h and Binder ratio Q_c, as obtained from the fits of the Monte Carlo data at $K = 0.935\,857$.

C	Q_p	χ	S_w	Q
$y_t = 1.34(1)$	$y_t = 1.337\,7(14)$	$y_h = 2.482\,2(2)$	$y_h = 2.4821(2)$	$Q_c = 0.914\,3(1)$

had described corrections by terms with b_i and b_2, where exponent y_i was fixed at -0.796 and y_2 was left free to be fitted. All the fits produced consistent results. The critical point was located at $K_c = 0.935\,856(2)$, the thermal exponent is $y_t = 1.336(3)$, and Binder ratio is $Q_c = 0.914\,2(1)$. The estimate of y_t is in good agreement with the existing results $y_t = 1.335(4)$.

According to the finite-size scaling theory, the specific heat behaves as $C = c_0 + aL^{2y_t-3}$ at criticality, where terms with amplitudes c_0 and a arise from the regular and the singular parts of the free energy density, respectively. The exponent $2y_t - 3$ is about -0.328, rather close to zero. This implies that terms with a and c_0 are difficult to be distinguished from each other in the fits of C. Thus, the specific heat C does not serve as a good candidate to determine the thermal exponent y_t. It turns out that quantity Q_p can be used to estimate y_t, since the finite-size scaling of Q_p at criticality reads $Q_p \propto L^{y_t}$. We fitted the data for Q_p by

$$Q_p(K,L) = L^{y_t}\left[\sum_{k=0}^{3} (K - K_c)^k L^{ky_t} + b_i L^{y_i} + b_1 L^{-2}\right]. \quad (8)$$

We obtain $K_c = 0.935\,855(2)$ and $y_t = 1.337\,5(15)$. The estimates of K_c and y_t agree with those obtained from ratio Q.

We also fitted the data for susceptibility $\chi = L^d \langle m^2 \rangle$ by

$$\chi(K,L) = L^{2y_h-3}\left[\sum_{k=0}^{3} (K - K_c)^k L^{ky_t} + b_i L^{y_i} + b_1 L^{-2}\right] \quad (9)$$

and obtain $K_c = 0.935\,856(2)$ and $y_h = 2.482\,0(2)$.

C. Data at criticality

Monte Carlo simulations were also performed right at $K = 0.935\,857$, consistent with the estimated critical point within one standard deviation. For the completeness of the present paper and the convenience for readers, we list in Table II the numerical data for specific heat C, susceptibility χ, Binder ratio Q, and quantity Q_p. The data for the average size of the Wolff clusters S_w per lattice site were already given in Table I. The size of a Wolff cluster is counted as the total number of lattice sites in the cluster, normalized by the volume of the lattice. Further, the data for C, and χ and S_w, and Q_p are plotted in Figs. 3–5, respectively.

As a consistency check, we fitted the data for C, χ, S_w, Q_p, and Q by

$$C(L) = c_0 + L^{2y_t-3}(a + b_i L^{y_i} + b_1 L^{-2}), \quad (10)$$

$$\chi(L) = x_0 + L^{2y_h-3}(a + b_i L^{y_i} + b_1 L^{-2}), \quad (11)$$

$$S_w(L) = L^{2y_h-6}(a + b_i L^{y_i} + b_1 L^{-2}), \quad (12)$$

$$Q_p(L) = L^{y_t}(a + b_i L^{y_i} + b_2 L^{y_2}) \quad (13)$$

and

$$Q(L) = Q_c + b_i L^{y_i} + b_2 L^{y_2}. \quad (14)$$

These formulas are relatively simple in comparison with those used in the previous subsection, since they do not include terms with $(K - K_c)$. The exponent y_2 was fixed at -1.96. The fits imply that the amplitudes b_i for quantities C, χ, S_w, and S_w are very small, and they cannot be used to estimate y_i. Thus, we fixed exponent y_i at -1.2. The results are given in Table III. As expected, these results are in good agreement with those obtained in the previous subsection.

TABLE IV. Summary of recent results for the critical point and renormalization exponents of the $O(4)$ model on the simple-cubic lattice. MC: Monte Carlo simulations, HT: high-temperature expansions, $d = 3$ PE: three-dimensional perturbative expansions.

Method	Reference	Year	K_c	y_t	y_h
MC	[6]	1995	0.936\,0(1)	1.337(16)	2.4871(11)
MC	[15]	1996	0.935\,90(5)		
MC	[3]	1996	0.935\,858(8)	1.329(2)	2.4808(6)
HT	[26]	1997		1.333(5)	2.483(5)
$d = 3$ PE	[4]	1998		1.350(11)	2.483(2)
ϵ-expansion	[4]	1998		1.357(15)	2.482(2)
MC	[8][a]	2000		1.353(4)	2.488(1)
MC	[7]	2001		1.335(4)	2.4817(5)
MC	Present	2006	0.935\,856(2)	1.337\,5(15)	2.4820(2)

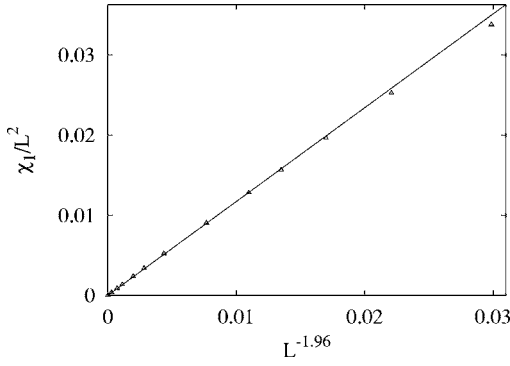[a]Simulations were only performed at $K = 0.935\,90$.

FIG. 6. Quantity χ_1/L^2 at the ordinary surface transition with $\kappa=-1$ vs $L^{-1.9596}=L^{2y_{h1}^{(o)}-4}$. The error bars are much smaller than the size of the data points.

Table IV gives a summary of some recent results for the bulk critical point and critical exponents of the $O(4)$ model. Our estimate of the critical point agrees well with those in Refs. [6,15,26], while the precision is significantly improved. Our results for the renormalization exponents y_t and y_h are most consistent with those in Ref. [7], in which Monte Carlo simulations were carried out for the $O(4)$-symmetric ϕ^4 model.

III. SURFACE PHASE TRANSITIONS

To investigate surface effects on the three-dimensional $O(4)$ model, we simulate the $O(4)$ model on the $L \times L \times L$ simple-cubic lattice with two open surfaces in the z direction. The nearest-neighbor coupling strength K_1 on the surfaces can take different values from K in the bulk. Wolff cluster simulations were performed at the estimated critical point $K_c=0.935\,856(2)$ for several values of K_1. In the remainder of the present paper, we denote the enhancement of surface couplings by parameter $\kappa=K_1/K-1$.

A. Ordinary surface transitions

For the Ising, XY, and Heisenberg models on the simple-cubic lattice, the special surface phase transitions occur [17,28–30] at $\kappa_c(N=1)=0.502\,14(8)$, $\kappa_c(N=2)=0.622\,2(3)$,
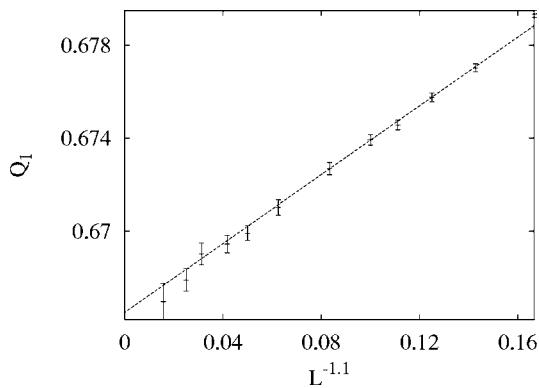

FIG. 7. Ratio Q_1 at the ordinary surface transition with $\kappa=-1$ vs $L^{-1.1}$. The exponent -1.1 was obtained from the fit.
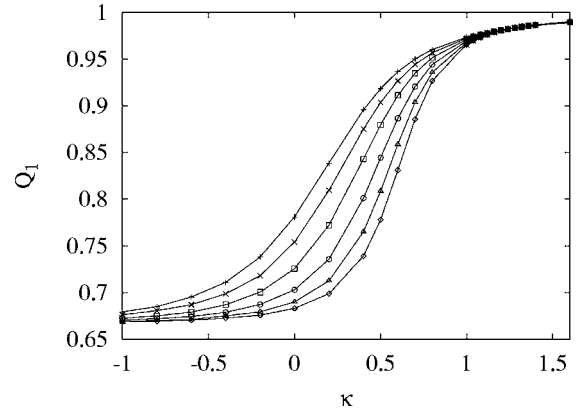

FIG. 8. Surface Binder ratio Q_1 in range $-1 \leqslant \kappa \leqslant 1.6$. The data points $+$, $\times$, $\square$, $\bigcirc$, $\triangle$, $\diamond$, and $*$ represent system sizes $L=6, 8, 12, 20, 32, 48$, and 64, respectively. The error bars of the data are smaller than the point sizes. The lines, which simply connect data points for each L, are just for illustration purpose.

and $\kappa_c(N=3)=0.85$. Thus, if the special transition also exists for the $O(4)$ model, one would expect it to occur at $\kappa_c > 0.8$; this will be confirmed later. For $\kappa < \kappa_c$, the surface phase transitions, i.e., the ordinary transitions, are in the same universality class. Further, the existing numerical data for the $O(N)$ model with $N \leqslant 3$ imply that the "fixed" point for the ordinary surface transition occurs at $\kappa < 0$; at this point, the amplitude for the leading finite-size corrections vanishes.

In the present work, we simulated at the ordinary surface transition of the $O(4)$ model with $\kappa=-1$; namely, the surface coupling strength K_1 was set at zero. The system size took 14 values in range $4 \leqslant L \leqslant 64$. For each system size, about 4×10^7 samples were generated. We sampled the magnetization density $\vec{m}_1$ on the surfaces and the associated moments, as

$$(\vec{m}_1)^k = \frac{1}{2}\left[\left(\frac{1}{L^d}\sum_{i:z=1}\vec{s}_i\right)^k + \left(\frac{1}{L^d}\sum_{i:z=L}\vec{s}_i\right)^k\right], \quad (15)$$

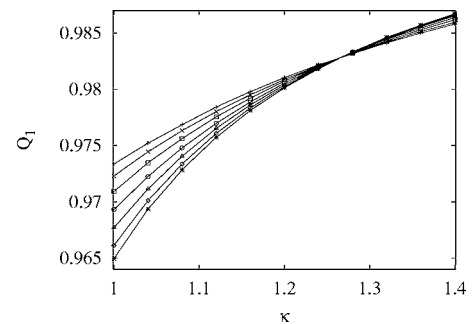where $k=2$ and 4. On this basis, we define the surface Binder ratio as

FIG. 9. Surface Binder ratio Q_1 in range $1 \leqslant \kappa \leqslant 1.4$. The data points $+$, $\times$, $\square$, $\bigcirc$, $\triangle$, $\diamond$, and $*$ represent system sizes $L=6, 8, 12, 20, 32, 48$, and 64, respectively. The error bars of the data are smaller than the point sizes. The lines, which simply connect data points for each L, are just for illustration purpose.
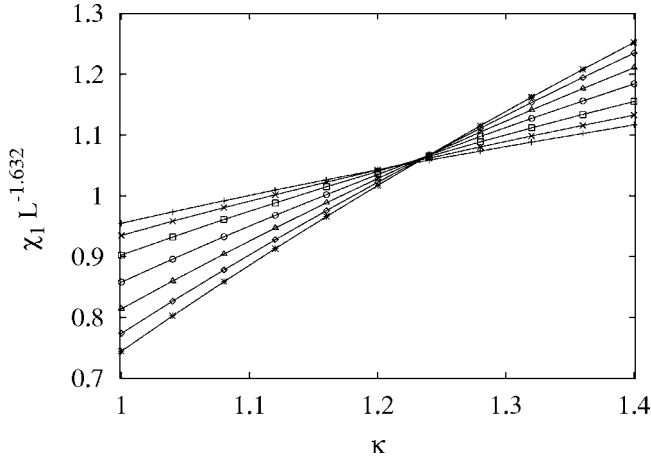
FIG. 10. Quantity $\chi_1 L^{2-2y_{h1}^{(s)}}$ in range $1 \leq \kappa \leq 1.4$. Exponent $y_{h1}^{(s)}$ was set at 1.816(2). The data points $+$, $\times$, $\square$, $\bigcirc$, $\triangle$, $\diamond$, and $*$ represent system sizes $L=6, 8, 12, 20, 32, 48,$ and 64, respectively. The error bars of the data are smaller than the point sizes. The lines, which simply connect data points for each L, are just for illustration purpose.

$$Q_1 = \frac{\langle (\vec{m}_1)^2 \rangle}{\langle (\vec{m}_1)^4 \rangle}. \qquad (16)$$

The data for the surface susceptibility $\chi_1 = L^2 \langle (\vec{m}_1)^2 \rangle$ and Q_1 are shown in Figs. 6 and 7, respectively. The fit of the data for Q_1 by

$$Q_1(L) = Q_{1c} + b_{i1} L^{y_{i1}} \qquad (17)$$

yields $Q_{1c} = 0.666\,7(6)$ and $y_{i1} = -1.1(1)$. Here, we have used exponent y_{i1} to describe the leading finite-size corrections at the ordinary surface transitions. From a simple scaling argument, it was derived [31] that the value of y_{i1} is -1, in agreement with our numerical estimate. On the other hand, one would also expect that the irrelevant exponent y_i for the bulk transition also exists at the ordinary transition. Again, the estimated value of y_{i1} is consistent with $y_i = -1.19(6)$, as determined earlier.

We then fitted the data for χ_1 by

$$\chi_1(L) = \chi_{1o} + L^{2y_{h1}^{(o)}-2}(a + b_i L^{y_{i1}} + b_1 L^{y_1}). \qquad (18)$$

The term with χ_{1o} arises from the analytical background. Exponent y_{i1} was fixed at -1. We simply took y_1 as -3 (we did not set $y_1 = -2$ because $2y_{h1}^{(o)} - 2 \approx 2$). The fit yields

$y_{h1}^{(o)} = 1.020\,2(12)$. To our knowledge, the value of $y_{h1}^{(o)}$ has not been reported yet.

B. Special surface transition

In order to see whether the special phase transition occurs for the critical $O(4)$ model in three dimensions, we performed simulations for several values of κ in range $-1 \leq \kappa \leq 1.6$. The system size took 12 values in range $6 \leq L \leq 64$. Parts of the data for Q_1 are shown in Fig. 8. This implies that the surface phase transitions for $\kappa < 0.7$ and for $\kappa > 1.4$ are in different universality classes, and a special transition must occur in between. Figure 9 shows the data for Q_1 in range $1 \leq \kappa \leq 1.4$. Indeed, a common intersection between the data lines for different sizes L is found to be near $\kappa = 1.26$. The existence of the special transition can be further demonstrated by the data for χ_1, which are shown in Fig. 10 as $\chi_1 L^{2-2y_{h1}^{(s)}}$ vs κ, with $y_{h1}^{(s)}$ fixed at 1.816, as determined later.

We fitted the Q_1 data in range $1 \leq \kappa \leq 1.4$ by Eq. (7), where m was taken as 6. After discarding the data for small system sizes $L \leq 8$, the Q_1 data can be well described by Eq. (7) with exponent $y_i = -2$. The fitting results are $\kappa_c = 1.258(8)$, $Q_{1c} = 0.982\,5(8)$, and $y_{t1}^{(s)} = 0.107(15)$. The value of $y_{t1}^{(s)}$ is rather close to 0.

However, the above results for κ_c and $y_{t1}^{(s)}$ cannot be taken too seriously, as argued in the following. From Figs. 8 and 9, it seems that, for $\kappa > 1.3$, the values of Q_1 do not converge to the low-temperature value 1. Instead, Q_1 seems to converge to a κ-dependent value. The overall behavior of Q_1 resembles that of the ratio Q for the bulk transitions in the Kosterlitz-Thouless universality class, as reported for the triangular Ising antiferromagnet with nearest- and next-nearest-neighbor interactions [32]. Thus, we cannot exclude the possibility that the special surface phase transition for the $O(4)$ model is Kosterlitz-Thouless-like. In particular, the small value $y_{t1}^{(s)} = 0.107(15)$ can be due to the fact that logarithmic correction terms are not included in Eq. (7). Nevertheless, from Fig. 9, it seems that the estimate $\kappa_c = 1.258(20)$ should be more or less reliable.

Taking into account the possible scenario that the special transition is Kosterlitz-Thouless-like, we did not fit all the χ_1 data by a single formula. Instead, we fitted the χ_1 data for a fixed value of κ by

$$\chi_1(L) = \chi_{1o} + L^{2y_{h1}^{(s)}-2}(a + b_1 L^{y_1} + b_2 L^{y_2} + b_3 L^{y_3}), \qquad (19)$$

where correction exponents were simply taken as $y_1 = -1$, $y_2 = -2$, and $y_3 = -3$. The results are shown in Table V. Linear

TABLE V. Results for y_{h1} from the fits by Eq. (19) for several values of κ. Symbol L_{min} represents the smallest system size of which the data were included in the fit.

κ	1.00	1.04	1.08	1.12	1.16	1.20
L_{min}	12	8	8	8	8	8
y_{h1}	1.728(4)	1.753(2)	1.768(2)	1.782(1)	1.795(1)	1.803(1)

κ	1.24	1.28	1.32	1.36	1.40	1.60
L_{min}	8	8	8	8	8	8
y_{h1}	1.812(1)	1.820(1)	1.828(1)	1.834(1)	1.841(1)	1.862(1)

interpolation between the values for $\kappa=1.24$ and $\kappa=1.28$ leads to $y_{h1}^{(s)}=1.86(2)$ for $\kappa_c=1.258(20)$.

IV. DISCUSSION

We performed extensive simulations for the $O(4)$ spin model on the simple-cubic lattice, and determined the bulk critical point and the associated renormalization exponents. The precision of our results, particularly that of the critical point, significantly improves over that of the existing results.

We also investigate surface effects on the critical $O(4)$ model in three dimensions, and observe a so-called special surface transition. Together with the results in Ref. [17], we conclude that, even though the two-dimensional $O(N)$ model with $N>2$ does not undergo phase transitions at nonzero temperature, the special surface transition still occurs when the surface couplings are sufficiently enhanced.

ACKNOWLEDGMENTS

[1] J. M. Carmona, A. Pelissetto, and E. Vicari, Phys. Rev. B **61**, 15136 (2000).

[2] Y. Deng and H. W. J. Blöte, Phys. Rev. E **68**, 036125 (2003), and references therein.

[3] H. G. Ballesteros, L. A. Fernandez, V. Martin-Mayor, and A. Munoz-Sudupe, Phys. Lett. B **387**, 125 (1996).

[4] R. Guida and J. Zinn-Justin, J. Phys. A **31**, 8103 (1998).

[5] M. Campostrini, M. Hasenbusch, A. Pelissetto, P. Rossi, and E. Vicari, Phys. Rev. B **65**, 144520 (2002).

[6] K. Kanaya and S. Kaya, Phys. Rev. D **51**, 2404 (1995).

[7] M. Hasenbusch, J. Phys. A **34**, 8221 (2001).

[8] J. Engels and T. Mendes, Nucl. Phys. B **572**, 289 (2000).

[9] A. Cucchieri and T. Mendes, J. Phys. A **38**, 4561 (2005).

[10] D. Toussaint, Phys. Rev. D **55**, 362 (1997).

[11] M. Hasenbusch, A. Pelissetto, and E. Vicari, Phys. Rev. B **72**, 014532 (2005).

[12] D. Loison, Physica A **271**, 157 (1999).

[13] A. Butti and F. P. Toldin, Nucl. Phys. **704**, 527 (2005).

[14] A. Pelissetto and E. Vicari, Phys. Rep. **368**, 549 (2002).

[15] M. Oevers, Diploma thesis, Bielefeld University, 1996.

[16] A. Cucchieri, J. Engels, S. Holtmann, T. Mendes, and T. Schulze, J. Phys. A **35**, 6517 (2002).

[17] Y. Deng, H. W. J. Blöte, and M. P. Nightingale, Phys. Rev. E **72**, 016128 (2005).

[18] K. Binder, in *Phase Transitions and Critical Phenomena*, edited by C. Domb and J. L. Lebowitz (Academic, London, 1987), Vol. 8, p. 1, and references therein.

[19] H. W. Diehl, in *Phase Transitions and Critical Phenomena*, edited by C. Domb and J. L. Lebowitz (Academic, London, 1987), Vol. 10, p. 76, and references therein.

[20] H. W. Diehl, Int. J. Mod. Phys. B **11**, 3503 (1997).

[21] M. Pleimling, J. Phys. A **37**, R79 (2004).

[22] Y. Deng and H. W. J. Blöte, Phys. Rev. E **71**, 016117 (2005).

[23] M. Krech, Phys. Rev. B **62**, 6360 (2000).

[24] U. Wolff, Phys. Rev. Lett. **62**, 361 (1989).

[25] U. Wolff, Phys. Lett. B **228**, 379 (1989).

[26] P. Butera and M. Comi, Phys. Rev. B **56**, 8212 (1997).

[27] K. E. Newman and E. K. Riedel, Phys. Rev. B **30**, 6615 (1984).

[28] D. P. Landau, R. Pandey, and K. Binder, Phys. Rev. B **39**, 12302 (1989).

[29] C. Ruge, A. Dunkelmann, F. Wagner, and J. Wulf, J. Stat. Phys. **73**, 293 (1993).

[30] C. Ruge and F. Wagner, Phys. Rev. B **52**, 4209 (1995).

[31] T. W. Burkhardt and J. L. Cardy, J. Phys. A **20**, L233 (1987).

[32] X. F. Qian and H. W. J. Blöte, Phys. Rev. E **70**, 036112 (2004).